Neutron radii of the calcium isotopes

W. R. Gibbs

Department of Physics, New Mexico State University, Las Cruces, New Mexico 88003
and Theoretical Division, Los Alamos National Laboratory, Los Alamos, New Mexico 87545

J.-P. Dedonder

Laboratoire de Physique Nucléaire, Université Paris VII, Paris, France
and Division de Physique Théorique, Institut de Physique Nucléaire, Orsay, France

We have analyzed pion scattering data to determine the proton and neutron radii of the calcium isotopes ^{40,42,44,48}Ca using model densities in which the neutron matter distributions are considered to have two components corresponding to core and valence neutrons. The proton radii determined agree with those obtained by electromagnetic means. The radii of the valence distributions show a monotonic decrease throughout the shell from $\sim$4.9 fm in ^{42}Ca to $\sim$4.4 fm in ^{44}Ca and $\sim$4.2 fm in ^{48}Ca, although this last case is only indicative. The large valence neutron radius of ^{42}Ca suggests that the ground state of this nucleus may have some characteristics of a bound dineutron orbiting a closed core.

PACS number(s): 21.10.Gv, 27.40.+z, 25.80.Dj

I. INTRODUCTION

The calcium isotopes have been used for many years as a laboratory for the study of the variations of nucleon density distributions across a shell. The charge radii [1], and their variation with neutron number [2], have been precisely measured. There is clear evidence that the changes observed in the charge radii are closely linked to variations in the distribution of the valence neutrons [3], in particular those exhibiting the even-odd effect which correlate with the pairing of the neutrons. While the *result* of the changing valence neutron distribution is clear, attempts to measure directly the neutron distributions themselves have met with only moderate success, in that the only radii which have been extracted to date [4, 5] are those of the total neutron density.

The present analysis relies primarily on the pion scattering data of Boyer *et al.* [6]. While these authors extracted the total neutron radii from their data, we have made a more detailed analysis of this same data using an improved scattering theory and a specific model of the nuclear density to obtain the valence- and core-neutron radii independently. We determine absolute neutron and proton radii separately in this analysis rather than fixing the proton value at that known from electromagnetic means. Since the proton radius obtained is in agreement with the electron scattering values, we have every reason to believe that the neutron radii have the same precision. Since the model that we use for the densities is the same as that often used for electron scattering analysis, we may expect that a major portion of the model dependence cancels as well.

For comparison proton radii we take from [1] (after removing the finite size of the proton and averaging among different determinations):

    40   3.360 ± 0.015 fm
    48   3.355 ± 0.010 fm.

The correction of Bertozzi *et al.* [7], due to the extra neutrons, would increase the radius of ^{48}Ca by 0.021 fm.

The differences in proton radii relative to ^{40}Ca [2] are shown in Table I.

II. METHOD OF ANALYSIS

We compare the prediction of a multiple-scattering theory (in the form of a two-body or "optical" potential) with π^+ and π^- elastic scattering data. The parameters of the scattering theory are held fixed and the nuclear densities varied to obtain the best χ^2. Cross sections were calculated as a function of two radii (the choice of the size of the mesh depending on the search) and a χ^2 surface was constructed. Such a χ^2 contour map is shown in Fig. 1. From each map a pair of radii was extracted with uncertainties based on the width of the ellipse. It is these statistical errors that are quoted in the tables presented in the next section.

Since no scattering theory (or data) is without fault, we made a series of variations of each to determine the effect on the radii obtained. It was observed that the resulting variation in the extracted radii, for the 180 MeV

TABLE I. Differences in proton radii, $R_p - R_p^{40}$. While we do not treat the odd isotopes or ^{46}Ca, those values are included to give an overall picture.

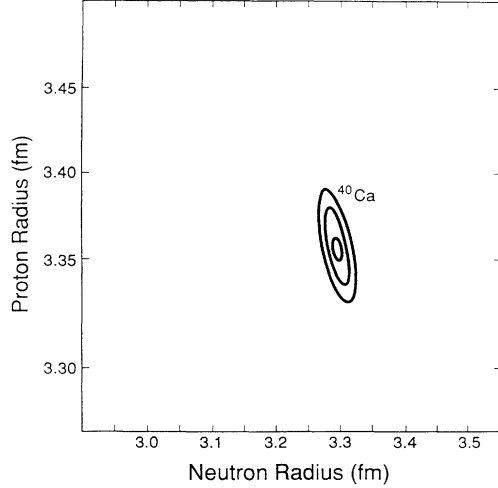|	
41	−0.002 ± 0.002
42	0.033 ± 0.002
43	0.017 ± 0.002
44	0.043 ± 0.002
45	0.019 ± 0.002
46	0.019 ± 0.001
47	0.001 ± 0.002
48	0.000 ± 0.001

FIG. 1. Contours for $\chi^2 = \chi^2_{min} + 1$, $\chi^2 = \chi^2_{min} + 4$, and $\chi^2 = \chi^2_{min} + 9$, i.e., for 1, 2, and 3 standard deviations from the minimum value for case A for ^{40}Ca and for proton vs neutron radii.

data, was relatively small, the quoted errors being a convolution of the uncertainties arising from this source with the statistical ones.

A. Densities

We present, along with analyses for the proton and total neutron radii, separate determinations of the "valence" and "core" neutron distributions. The present analysis is carried out within a specific model for the nuclear density [8]. A reference "core" proton density is first constructed to represent the proton density of ^{40}Ca. Solutions for single-particle wave functions in a Woods-Saxon potential well are calculated in order to construct a nuclear density composed of the squares of the wave functions with $2\ell + 1$ weighting. The radius of the well is taken as $1.31A^{1/3}$ fm, the diffuseness as 0.5 fm, and a Coulomb potential (due to a uniformly charged sphere) is used. The potential depths for the different orbitals are varied in order to obtain the best fit to the measured charge density (after including the size of the proton).

The corresponding reference neutron density is obtained by recalculating the wave functions without the Coulomb potential. The neutrons are found to be bound more strongly than the protons, as observed experimentally. Since the proton density is more extended than that of the neutrons, due to the smaller binding energy, the proton radius is greater than that of the neutrons. The procedure described above results in a difference in radii of $R_p - R_n = 0.15$ fm. Of course such a calculation assumes that the neutrons and protons move in exactly the same potential well. Since the n-p force is more attractive than the n-n (or p-p) force, the protons actually move in a more compact potential than the neutrons, hence it is expected that the true difference in the radii is less than this naive estimate.

The valence neutron density is also calculated in a well with a radius of $1.31(A - 1)^{1/3}$ with the depth of the

potential chosen to give the correct binding energy for the last neutron. We assume a pure $\ell=3$ configuration.

Using the functional form supplied by these three reference densities, the rms radii are varied by scaling the radial variable while maintaining the proper normalization. An optical potential is constructed, as described below, based on each of these densities, the total effective pion-nucleus two-body interaction being taken as the sum of the three (two for ^{40}Ca) individual potentials.

B. Reactive content

The quasifree part of the (first order) optical potential is calculated by the technique of Ref. [9] based on a number of studies of pion scattering [10]. We use a finite-range optical potential solved in coordinate space by standard numerical procedures. Although it is the same method used in Ref. [9], we briefly review it here.

The form of the potential in coordinate space for a given pion-nucleus partial wave, L, is given by

$$V_L(r, r') = b_{0L} u_{0L}(r, r') + b_{1L} u_{1L}(r, r') \tag{1}$$

where

$$\sum_L u_{0L}(r, r') P_L(x)$$

$$= \int d\mathbf{q}\, d\mathbf{q}'\, e^{i\mathbf{q}\cdot\mathbf{r} - i\mathbf{q}'\cdot\mathbf{r}'} v(q) v(q') \rho(|\mathbf{q} - \mathbf{q}'|) \tag{2}$$

and

$$\sum_L u_{1L}(r, r') P_L(x)$$

$$= \int d\mathbf{q}\, d\mathbf{q}'\, e^{i\mathbf{q}\cdot\mathbf{r} - i\mathbf{q}'\cdot\mathbf{r}'} v(q) v(q') \mathbf{q} \cdot \mathbf{q}' \rho(|\mathbf{q} - \mathbf{q}'|). \tag{3}$$

Here $\rho(s)$ is the Fourier transform of the density and x is the cosine of the angle between $\mathbf{r}$ and $\mathbf{r}'$. The off-shell form factor function, $v(q)$, is taken to be

$$v(q) = \frac{\alpha^2 + k^2}{\alpha^2 + q^2}. \tag{4}$$

The strengths, b_{0L} and b_{1L}, carry the index of the pion-nucleus partial wave since the t matrix has been corrected for medium effects, including Pauli blocking, according to the methods of Ref. [9]. Since there is a modification of the off-shell range (the range of the pion-nucleon interaction) due to the propagation of the intermediate composite system, the value to be used in nuclear scattering may differ from that in free space. We found empirically (independently for each of the eight cases) that the best value was near 550 MeV/c in reasonable agreement with that expected [9].

Pion "true" absorption was parametrized by a purely imaginary constant (iW) multiplying the square of the density. The strength was estimated [11] from pion-absorption cross sections but only a crude value is obtainable by these means. Thus we consider the variation of this parameter as described below.

We considered two isospin-breaking effects; the energy shift due to the Coulomb potential and virtual Coulomb excitation. For the first, a simple shift of ± 9 MeV was applied to the energy used in the calculation of the strengths b_{0L} and b_{1L}. There has already been an extensive investigation of the importance of this correction [12]. The Coulomb excitation corrections were made with the methods of [13]. While the calculations made with this effect included might be expected to be the most accurate, since it is probably an overestimate, its inclusion (or not) was treated as an error estimator.

C. Treatment of the data

The data were usually restricted to angles before the third maximum with the idea that data at high momentum transfer give information on physical quantities other than the rms radii. Of course, since this analysis is restricted to the resonance region, only the surface of the nucleus is being probed and data at larger angles would presumably give more detailed information on the shape of the density and on the scattering theory, both of which are beyond the scope of the present work.

The errors quoted in the published data are statistical only. Upon reading details presented in Ref. [6] some estimate of realistic errors can be obtained. The author states that, in particular for the forward angles, the data points were found to be reproducible only to the order of 5%. In attempting to pass a smooth curve through the data at larger angles it is also found that points are consistent with adjacent points only to the order of 5% (except for the case of ^{42}Ca which is worse as discussed below). For this reason we have added to the quoted errors (in quadrature) an additional 5% of the value at each point. Note that the statistical errors are smaller than 5% only where the cross section is large (near the maxima) and larger than 5% where the cross section is small (in the minima). Since it is the position of the minima which determine (primarily) the radii, this convolution has little effect on the values obtained (see the discussion for ^{42}Ca in this regard).

Since the normalization of the data was uncertain to about 10%, it was considered as a parameter. Other treatments of the data specific to given cases are discussed below.

III. RESULTS

The principal variations in the scattering model of Sec. II B are identified with a letter. A represents the "standard" case (in the sense that all other calculations are made with only one condition different from it) has an *a priori* specified normalization (different for each isotope and pion charge), the interaction strengths for the valence neutrons are calculated with free pion-nucleon phase shifts, no Coulomb excitation is included, the true absorption has the value estimated from the absorption experiments (as described above) and the off-shell range is 550 MeV/c. In case B the data normalization is changed from the standard value (1.10 in all cases except π^+ on ^{42}Ca where it is 1.0) to 1.05. In case C the valence nucleons are treated with medium corrected interaction strengths. The condition corrected/free only concerns valence neutrons, core nucleons always being treated with corrected strengths. Presumably the most appropriate treatment for the valence neutrons is to adopt "free" strengths (except for ^{48}Ca) since the blocking and shifts are always computed for a closed shell, but due to the uncertainty in this condition we treat this possibility as an error estimator. In case D the Coulomb excitation potential calculated in Ref. [13] is included. For the case E the true-absorption coefficient is increased by 25% from the value expected [11] from the true-absorption experiments. In case F the off-shell range is taken to be 650 MeV/c. The standard value of 550 MeV/c was obtained from a global study of the χ^2 for all the isotopes of calcium considered. While there were differences in some cases this value was acceptable (in a χ^2 sense) for all data sets.

The radii extracted for each of the isotopes are given in Tables II to IX. With the exception of ^{42}Ca it was not possible to extract a proton radius from the π^- data, the χ^2 being essentially independent of this quantity. In those cases in which a proton radius can be obtained it agrees with the known electromagnetically determined values [1,2], within errors. We emphasize that we do not need to use the electron-scattering values as input; an independent determination of the radii made with pion scattering gives agreement with those already known.

We make a determination of the "core" (R_c) and "valence" (R_v) neutron radii separately by setting the proton radius to the known value and considering χ^2 as a function of these two variables. The uncertainties are larger,

TABLE II. Radii extracted from π^- scattering on ^{40}Ca and the combined analysis. A similar table for π^+ scattering exists but is not shown.

| | π^- | | Combined analysis | | |
	R_n^{40}	χ^2/N	R_p^{40}	R_n^{40}	χ^2/N
A	3.29 $\pm$ 0.01	3.08	3.34 $\pm$ 0.03	3.31 $\pm$ 0.03	1.99
B	3.29 $\pm$ 0.02	4.19	3.35 $\pm$ 0.03	3.31 $\pm$ 0.01	2.39
D	3.28 $\pm$ 0.01	3.05	3.41 $\pm$ 0.03	3.28 $\pm$ 0.02	1.69
E	3.28 $\pm$ 0.02	3.29	3.35 $\pm$ 0.03	3.31 $\pm$ 0.02	1.76
F	3.30 $\pm$ 0.01	3.06	3.35 $\pm$ 0.03	3.32 $\pm$ 0.02	2.07
Average	3.29 $\pm$ 0.02		3.36 $\pm$ 0.04	3.31 $\pm$ 0.03	

TABLE III. Radii obtained from π^- scattering on ^{42}Ca. The $R_p - R_n$ analysis was performed with 10% errors. The total neutron radius obtained from combining R_c and R_v is 3.33 fm.

	5%			Selected data		
	R_c^{42}	R_v^{42}	χ^2/N	R_c^{42}	R_v^{42}	χ^2/N
A	3.12 ± 0.02	4.82 ± 0.07	3.63	3.12 ± 0.02	4.93 ± 0.10	3.41
B	3.13 ± 0.03	5.07 ± 0.07	3.98	3.12 ± 0.02	5.10 ± 0.10	3.80
C	3.16 ± 0.02	4.93 ± 0.10	3.38	3.16 ± 0.02	4.95 ± 0.12	3.30
D	3.10 ± 0.04	4.86 ± 0.11	3.52	3.12 ± 0.02	4.88 ± 0.12	3.28
E	3.10 ± 0.04	4.97 ± 0.10	3.84	3.12 ± 0.02	4.98 ± 0.12	3.71
F	3.13 ± 0.04	4.84 ± 0.08	3.82	3.12 ± 0.02	4.90 ± 0.10	3.56
Average	3.13 ± 0.04	4.91 ± 0.13		3.13 ± 0.02	4.95 ± 0.15	

	10%				
	R_p^{42}	R_n^{42}	R_c^{42}	R_v^{42}	χ^2/N
A	3.38 ± 0.07	3.32 ± 0.02	3.12 ± 0.02	4.86 ± 0.12	1.47
B	3.34 ± 0.10	3.35 ± 0.03	3.11 ± 0.02	5.02 ± 0.10	1.74
C	3.48 ± 0.08	3.32 ± 0.03	3.16 ± 0.02	4.88 ± 0.14	1.42
D	3.35 ± 0.13	3.32 ± 0.02	3.12 ± 0.02	4.80 ± 0.10	1.40
E	3.36 ± 0.13	3.33 ± 0.03	3.12 ± 0.02	4.95 ± 0.14	1.63
F	3.45 ± 0.10	3.31 ± 0.03	3.13 ± 0.02	4.87 ± 0.13	1.53
Average	3.39 ± 0.12	3.32 ± 0.03	3.13 ± 0.02	4.90 ± 0.13	

TABLE IV. Radii from the analysis of π^+ scattering on ^{42}Ca. The total neutron radius from combining R_v and R_c is 3.28 fm. The electromagnetic value for the proton radius is 3.388±0.010 fm.

	R_p^{42}	R_n^{42}	χ^2/N	R_c^{42}	R_v^{42}	χ^2/N
A	3.35 ± 0.02	3.33 ± 0.04	1.05	3.05 ± 0.02	4.78 ± 0.12	1.04
B	3.35 ± 0.04	3.28 ± 0.04	1.24	3.08 ± 0.03	4.35 ± 0.10	1.22
C	3.37 ± 0.02	3.30 ± 0.06	1.22	3.08 ± 0.04	4.62 ± 0.16	1.21
D	3.41 ± 0.02	3.36 ± 0.05	1.92	3.18 ± 0.03	5.32 ± 0.13	1.91
E	3.35 ± 0.02	3.36 ± 0.06	1.16	3.05 ± 0.03	4.97 ± 0.10	1.06
F	3.41 ± 0.01	3.25 ± 0.02	1.36	3.10 ± 0.04	4.78 ± 0.14	1.38
Average	3.37 ± 0.03	3.33 ± 0.05		3.09 ± 0.05	4.80 ± 0.32	

TABLE V. Radii obtained from a combined analyses of π^+ and π^- scattering on ^{42}Ca. The total neutron radius from combining R_v and R_c is 3.32 fm.

	R_p^{42}	R_n^{42}	χ^2/N	R_c^{42}	R_v^{42}	χ^2/N
A	3.36 ± 0.02	3.33 ± 0.03	1.26	3.10 ± 0.02	4.90 ± 0.10	1.45
B	3.35 ± 0.03	3.33 ± 0.03	1.65	3.10 ± 0.01	4.88 ± 0.10	1.95
C	3.37 ± 0.03	3.34 ± 0.04	1.56	3.14 ± 0.02	4.87 ± 0.21	1.66
D	3.41 ± 0.03	3.32 ± 0.03	1.94	3.13 ± 0.02	4.98 ± 0.10	2.14
E	3.36 ± 0.02	3.34 ± 0.03	1.40	3.10 ± 0.02	5.00 ± 0.10	1.43
F	3.38 ± 0.03	3.33 ± 0.03	1.48	3.13 ± 0.02	4.80 ± 0.12	1.50
Average	3.37 ± 0.03	3.33 ± 0.03		3.12 ± 0.02	4.90 ± 0.15	

TABLE VI. Radii obtained from the analysis of π^+ scattering on ^{44}Ca. The electromagnetic value for the proton radius is 3.398±0.010 fm. The total neutron radius from combining R_v and R_c is 3.44 fm.

	R_p^{44}	R_n^{44}	χ^2/N	R_c^{44}	R_v^{44}	χ^2/N
A	3.37 ± 0.02	3.44 ± 0.03	0.82	3.14 ± 0.03	4.48 ± 0.10	0.80
B	3.37 ± 0.01	3.50 ± 0.02	0.79	3.11 ± 0.02	4.74 ± 0.05	0.77
C	3.42 ± 0.02	3.36 ± 0.04	1.06	3.25 ± 0.04	4.20 ± 0.12	1.06
D	3.41 ± 0.01	3.49 ± 0.02	1.17	3.23 ± 0.05	4.75 ± 0.12	1.18
E	3.37 ± 0.01	3.47 ± 0.02	0.74	3.14 ± 0.05	4.59 ± 0.09	0.73
F	3.41 ± 0.01	3.41 ± 0.02	1.02	3.21 ± 0.03	4.45 ± 0.07	1.03
Average	3.39 ± 0.03	3.45 ± 0.04		3.18 ± 0.08	4.54 ± 0.21	

TABLE VII. Radii obtained from the combined analysis for ^{44}Ca. The total neutron radius from R_c and R_v is 3.43 fm.

	R_p^{44}	R_n^{44}	χ^2/n	R_c^{44}	R_v^{44}	χ^2/N
A	3.38 ± 0.03	3.42 ± 0.02	1.11	3.19 ± 0.05	4.42 ± 0.10	1.11
B	3.37 ± 0.03	3.43 ± 0.02	1.14	3.15 ± 0.04	4.52 ± 0.10	1.10
C	3.40 ± 0.04	3.42 ± 0.03	1.64	3.24 ± 0.04	4.30 ± 0.15	1.52
D	3.43 ± 0.04	3.41 ± 0.02	1.42	3.20 ± 0.04	4.37 ± 0.15	1.68
E	3.38 ± 0.03	3.42 ± 0.02	1.04	3.17 ± 0.03	4.47 ± 0.10	1.04
F	3.40 ± 0.04	3.42 ± 0.02	1.31	3.23 ± 0.04	4.32 ± 0.10	1.25
Average	3.39 ± 0.04	3.42 ± 0.02		3.20 ± 0.04	4.40 ± 0.15	

of course, but the numbers extracted are very interesting nonetheless.

With a fixed proton radius we can also make a contour plot of the χ^2 for the total neutron radius versus the core radius. This third method of analysis gives the most accurate determination of the total neutron radius.

A. ^{40}Ca

The data for both π^+ and π^- were used through 63.41°, which is just past the second minimum. Figure 1 shows the χ^2 contour obtained with a combination of the π^+ and π^- data for case A below.

A value can be extracted for both a neutron and proton radius from π^+ and a neutron radius from π^-. Summing the two χ^2, thus requiring a simultaneous fit to π^+ and π^- under the same conditions, a combined analysis results and is also presented in Table II. In this case the π^- scattering data play a role in determining the proton radius. In a preliminary version of this analysis, we reported [14] a value of the difference in proton-neutron radius for ^{40}Ca of the order of 0.1 fm. From Table II above one sees that the analysis from the combined χ^2 gives $R_p^{40} - R_n^{40} = 0.05 \pm 0.05$ fm. The most complete calculation from the theoretical point of view might be thought to be that with Coulomb excitation included giving 0.13±0.04 fm. This large difference is obtained by raising the proton radius outside of the limits determined by electron scattering leading us to believe that the Coulomb excitation correction used is an overestimate of the effect as already noted [13]. From the separate analyses one has $R_p = 3.38\pm0.04$ fm (π^+) and $R_n = 3.29\pm0.02$ fm (π^-) yielding a difference of 0.09±0.04 fm. While values in

the region 0.1 fm are very possible, the combined analysis probably gives the most accurate value of this difference. This last result (0.05±0.05 fm) is in agreement with the theoretical value of 0.05 fm found by several authors [15-17]. It is in contradiction with the recent large radius difference (0.2–0.3 fm) extracted from proton scattering by Ray [18] who interprets this discrepancy as a measure of the error of the nonrelativistic impulse approximation for proton-nucleus scattering.

B. ^{42}Ca

The data were used to 66.43° for π^+ and to 57.39° for π^-. In this second case the angular distribution is only entering into the second minimum. Figure 2 shows the contour plot for the combined analysis for case A.

The data points of Boyer et al. [6] for π^- scattering on ^{42}Ca show a larger spread than seen in the other isotopes, making it impossible to obtain a reasonable value of χ^2 under the same conditions as the other cases treated. In an attempt to see if this variation in the value of χ^2 affected the neutron radius obtained, some modifications of the data were considered. First the points with obviously large deviations were removed. The results are shown in Table III under the title of "selected data." As can be seen there is little change in the nucleon radii extracted. It is also clear that there is not much improvement in the χ^2. A closer inspection shows that the same problem remains, i.e., there are regions in angle where two adjacent points have a very different χ^2 (e.g., zero and twenty).

In this case it is not possible to fit the data with any smooth curve. For this reason we also tried increasing the error by convoluting 10% of the cross section instead

TABLE VIII. Radii obtained from π^- scattering on ^{48}Ca. The total neutron radius from combining R_v and R_c is 3.45 fm.

	43 points R_n^{48}	χ^2/N	50 points R_n^{48}	χ^2/N	R_c^{48}	R_v^{48}
A	3.50 ± 0.03	1.09	3.45 ± 0.02	1.75	3.16 ± 0.05	4.10 ± 0.08
B	3.51 ± 0.04	1.13	3.44 ± 0.02	1.89	3.07 ± 0.07	4.23 ± 0.05
C	3.47 ± 0.02	1.62	3.47 ± 0.02	2.04	3.36 ± 0.05	3.75 ± 0.15
D	3.50 ± 0.02	1.10	3.45 ± 0.02	1.61	3.14 ± 0.05	4.07 ± 0.05
E	3.52 ± 0.03	1.15	3.44 ± 0.03	1.86	3.12 ± 0.05	4.15 ± 0.05
F	3.52 ± 0.02	1.06	3.43 ± 0.03	1.55	3.40 ± 0.05	3.70 ± 0.06
Average	3.50 ± 0.04		3.45 ± 0.03		3.21 ± 0.13	4.00± 0.22

TABLE IX. Radii obtained from the combined analyses for ^{48}Ca. The total neutron radius from combining R_c and R_v is 3.41 fm. For case F the ambiguity in the $R_c - R_v$ plane was so severe that no values are quoted.

	R_p^{48}	R_n^{48}	χ^2/N	R_c^{48}	R_v^{48}	χ^2/N
A	3.30 ± 0.02	3.43 ± 0.01	2.52	3.04 ± 0.08	4.20 ± 0.10	3.01
B	3.30 ± 0.02	3.44 ± 0.01	2.69	2.94 ± 0.08	4.30 ± 0.10	2.95
C	3.33 ± 0.02	3.42 ± 0.02	2.80	3.13 ± 0.05	4.05 ± 0.10	2.62
D	3.36 ± 0.03	3.42 ± 0.02	3.37	3.04 ± 0.06	4.20 ± 0.10	3.40
E	3.30 ± 0.01	3.44 ± 0.01	2.68	3.00 ± 0.07	4.25 ± 0.10	2.98
F	3.33 ± 0.02	3.43 ± 0.02	3.11			
Average	3.32 ± 0.03	3.43 ± 0.02		3.03± 0.09	4.20± 0.13	

of the usual 5%. The results are shown in Table III under the heading "10%." The effect on the values of the radii extracted is seen to be very small.

Note that the core neutron radius is found to be small and the valence radius large consistently for both signs of pion, i.e., for two independent data sets. For the proton-neutron analysis R_c^{42} was taken to be 3.129 fm and for the core-valence analysis R_p^{42} was 3.387 fm.

C. ^{44}Ca

The data for both π^+ and π^- were used to 70.44° which is just past the second minimum. Figure 2 shows the combined analysis for case A. The value of R_c^{44} was 3.185 fm for the proton-neutron analysis and R_p^{44} was 3.387 fm for the core-valence analysis. The core radius is slightly larger than for ^{42}Ca, as might be expected from the electromagnetic determinations for the proton radii, but the valence radius is noticeably smaller. The π^- analysis displays no anamolous features and is not shown.

D. ^{48}Ca

The π^+ data were used through 65.42° and the π^- through 70.44° (corresponding to 50 points), both past the third maximum. Figure 2 shows the χ^2 from the combined analysis of A.

An analysis for R_c and R_v for π^- redone with 43 data points yields very different results with large core (3.5 fm on the average) and small valence radii (smaller than 3.5 fm) with a χ^2 of the order 1.1. The problem is that there is a long valley going across the (R_c, R_v) plane from the lower corner on the right (near $R_c=3.53$ and $R_v=3.40$) to the minimum shown in Fig. 2. The origin of this ambiguity is unknown, it may lie in the model chosen or in the quality of the data. While the second minimum leads to unphysical values of the neutron radii, its influence on the first minimum may not be negligible because of the effective extention of the χ^2 ellipse. Hence we are cautious about quoting errors in the R_c and R_v variables along the major axis of the ^{48}Ca ellipse in Fig. 2.

The total neutron radius for ^{44}Ca is seen to be the same as that for ^{48}Ca which implies (since there are twice as many valence neutrons in ^{48}Ca as in ^{44}Ca) that either the core neutron radius or the valence neutron radius in ^{48}Ca has decreased over that in ^{44}Ca (or a combination

of the two). We see that the core radius has remained almost constant (possibly decreasing somewhat) but that there is a sizable decrease in the valence neutron radius.

IV. CONCLUSIONS

A. Valence neutron distributions

For ^{42}Ca we observe a large radius for the valence neutron system. In retrospect it is perhaps natural to expect a larger radius from the electromagnetic data on the proton distributions, since R_p is increased almost as much (beyond that of ^{40}Ca) as that of ^{44}Ca with only two neutrons "pulling" instead of four. Figure 3 shows the valence neutron densities normalized to an integral of 1. It is interesting to compare with the difference distributions (^{4n}Ca$-^{40}$Ca) obtained from alpha-particle scattering, Fig. 4 of Ref. [5]. There it is also clear that the
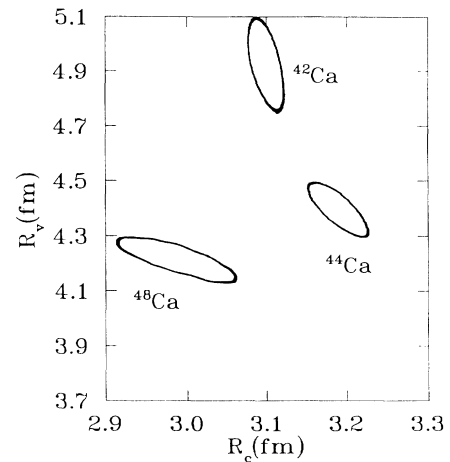
FIG. 2. Contours for $\chi^2 = \chi^2_{\min} + 4$, i.e., for 2 standard deviations from the minimum value for case A and for ^{42}Ca, ^{44}Ca, and ^{48}Ca. For the ^{48}Ca case there is a second minimum to the right of the figure and near the bottom axis which effectively extends the valley of the χ^2 surface so that no precise values of the valence and core radii can be given. It is clear none the less that the valence radius of ^{42}Ca is larger than the other two. Also notable is the decrease in the neutron core radius compared with the neutron radius of ^{40}Ca (at least for ^{42}Ca and ^{44}Ca).
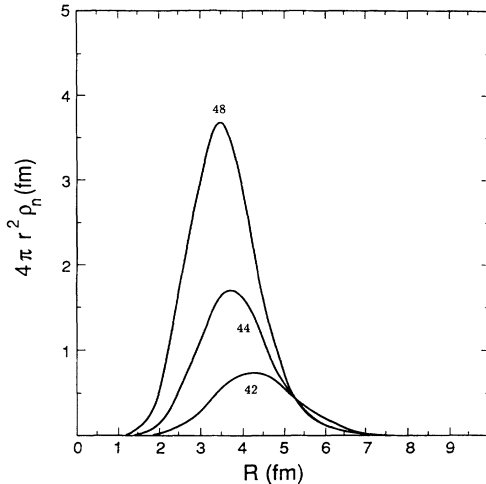
NEUTRON RADII OF THE CALCIUM ISOTOPES

FIG. 3. Valence neutron densities (multiplied by r^2) for ^{42}Ca, ^{44}Ca, and ^{48}Ca showing the shift in the peak position as a function of isotope.

excess neutron density peaks at larger values of radii for ^{42}Ca than for ^{48}Ca.

Consider the following scenario for understanding this behavior. Starting from a pure $f_{7/2}$ configuration for the valence neutrons, the seniority model gives an exact representation of the valence neutron wave functions. In this model ^{42}Ca shows a very high degree of "positive" correlation between the two valence neutrons, i.e., they are considerably more likely to be found near to one another than in a simple product density. A given pair of neutrons in ^{44}Ca is less likely to be found near each other than in ^{42}Ca but still more likely than in a product density. For ^{48}Ca the wave function is represented by a Slater determinant resulting in an anticorrelation of the neutrons, being *less* likely to be found close together than in a product density. Thus, if we consider that the binding energy is made up of the interaction with the mean field (mostly the core nucleons) and the "residual" interaction among pairs of neutrons, the contribution (per neutron) of the potential acting between pairs of neutrons becomes less important as we progress through the shell.

Since the binding energy of the last (even) neutron remains essentially constant throughout the shell, there must be more interaction with the core as the number of valence neutrons increases, and hence a more compact wave function. Thus the interaction among the pairs of neutrons plays a crucial role in determining the nuclear state vector.

This idea is neither new nor unique to this nucleus. Migdal [19] discussed the idea of the attractive nuclear potential aiding in the binding of a dineutron state and it has recently created a great deal of interest in the case of ^{11}Li. In this case the last two neutrons are thought [20] to form a halo and have a very large radius, as determined from calculations [21, 22], measurements of interaction cross sections [23], and momentum distributions from the dissociation of beams of ^{11}Li [24, 25]. Numbers as large as 9 fm have been quoted for this radius [25] but a recent

TABLE X. Best values of the neutron radii obtained by combining the π^+ and π^- data and fixing the proton radius. Because of the ambiquity for π^- scattering on ^{48}Ca mentioned in Sec. III D this method did not yield a better value for the total neutron radius for this isotope so no values are shown.

	^{42}Ca	^{44}Ca
A	3.31± 0.01	3.41± 0.01
B	3.31± 0.01	3.43± 0.03
C	3.33± 0.03	3.44± 0.01
D	3.33± 0.02	3.42± 0.01
E	3.32± 0.01	3.41± 0.02
F	3.32± 0.01	3.44± 0.02
Average	3.32± 0.02	3.43± 0.02

measurement [26] and analysis [27], using pion double-charge exchange, indicate that the radius is very unlikely to be larger than 6 fm.

The two-neutron clustering in ^{42}Ca may be expected to be less pronounced than in ^{11}Li but has significant consequences for other reactions. For certain cases, in pion double-charge exchange (DCX) at resonant energies, the minimum in the angular distribution is located at a value which is apparently too small to be explained by diffractive theories. The cases in point are analog transitions in "closed-shell-plus-2-neutron" nuclei, notably ^{18}O [27] and ^{42}Ca [28]. The calculations used for comparison were made with "traditional" values for the rms radius of the two neutrons (e.g., around 4.0 fm for ^{42}Ca) [29]. We have verified that, for the two-neutron wave functions obtained in the present work, the angle of the minimum for pion DCX does indeed fall at the experimentally observed position. The shape of the angular distribution is
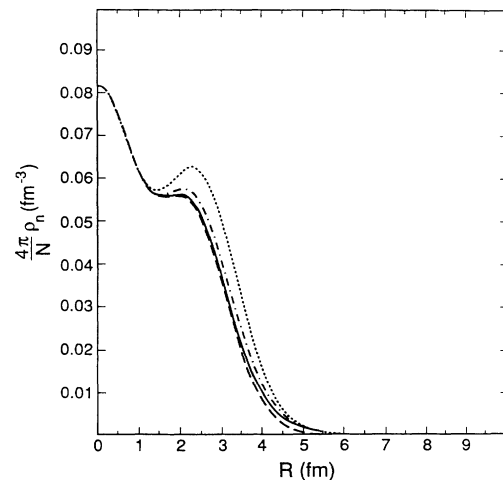

FIG. 4. Total neutron densities for the calcium isotopes. The dashed curve corresponds to ^{40}Ca, the solid to ^{42}Ca, the dash-dotted to ^{44}Ca, and the dotted to ^{48}Ca. The large rise in density at small r is given by the model used and the present work has nothing to say about its validity. It is only the surface region that is sampled by the pion probe at resonance energies and the form of the density inside of 3 fm depends on the model used.

TABLE XI. Summary of total neutron and proton radii.

| | R_p | | R_n | $R_n - R_p$ | |
	Present work	E/M		Present work	Decharge/Gogny
40	3.36 ± 0.03	3.360 ± 0.015	3.31 ± 0.03	-0.05 ± 0.04	-0.04
42	3.37 ± 0.03	3.388 ± 0.010	3.33 ± 0.03	-0.04 ± 0.04	$+0.01$
44	3.39 ± 0.04	3.398 ± 0.010	3.42 ± 0.02	$+0.03 \pm 0.04$	$+0.06$
48	3.32 ± 0.03	3.355 ± 0.010	3.43 ± 0.02	$+0.11 \pm 0.04$	$+0.14$

poorly matched to the data but this defect may be related to the fact that the shape of the radial distribution will be altered because the neutron-neutron interaction will yield a transition density with a form not derivable from a Woods-Saxon potential.

B. Total neutron distributions

In order to obtain the best value of the total neutron radii a different strategy was adopted than those followed in the preceeding analyses. Up until now we have attempted to extract the proton and neutron radii independently to prove consistency with the proton densities obtained by electromagnetic means. Once we have convinced ourselves that the analysis is consistent we may use the electromagnetic values to reduce the errors on the total neutron radii. The analysis consists of choosing the proton radius and varying the valence and core neutron distributions but looking only at the total neutron radius as a function of the assumed core value using the combined χ^2. Table X shows the values obtained in this manner. The radii are completely consistent with those listed in the other tables but the errors are reduced.

Figure 4 shows the total neutron densities obtained. Since only the surface is sampled in pion scattering at resonance energies, the shape in the interior is determined by the form of the independent particle model densities. The peak in the density in the surface for ^{48}Ca was also observed in alpha scattering [5].

From Table XI we note that the differences in the total neutron and proton radii are in basic agreement with the Hartree-Fock-Bogoliubov calculations of Decharge and Gogny [16]. The proton scattering analyses have given a variety of values [30–33], for example, for the difference in the neutron-proton radii for ^{48}Ca from 0.23 fm of Ref. [30] to 0.09 fm of Ref. [31]. There is one possible discrepancy, that of ^{42}Ca. It is interesting to note that although the valence neutron radius is large, the total neutron radius seems to be small, corresponding to a very small core radius. While this might be a physical effect, it may also be due to the form chosen for the density of the two valence neutrons. If there is indeed clustering, as discussed in Sec. IV A, the true radial distribution would be more concentrated at larger values of radius than the presently assumed solution in a Woods-Saxon well. Since the variations made in the current analysis do not allow for the possibility of changing this shape, the only way to lower the density in the intermediate surface region is to reduce the radius of the neutron core. While this lowers the density on the surface, it may lead to an erroneous rms radius since the assumption of the shape of single

particle densities is not correct.

While small χ^2 values speak for themselves, it is instructive to see directly what effect a radius variation has on the comparison with data. To this end we show (Fig. 5) a comparison of two different total neutron radii for π^- scattering on ^{44}Ca. The solid curve shows the calculation (under conditions A) with a radius 3.43 fm, essentially our central value. The dashed curve shows the calculation resulting from an increase of 2% to 3.49 fm. The difference due to a change of 1% is clearly visible on a full-size plot but 2% was used for the presented figure.

We also looked briefly at the data from the same experiment at 116 MeV but the theoretical uncertainties, as judged from model variations similar to those defined in Sec. III, were found to be larger by about a factor of 2. Both neutron and proton radii have a tendency to be larger than those in the analysis at 180 MeV (and in electron scattering) but the discrepancy is considerably less than in the original analysis by Boyer et al. [6]. While there is a greater sensitivity to the Pauli blocking (the effect is stronger at lower energies) and to the off-shell range, we believe that a large part of the dificulty comes from the treatment of true absorption. At 116 MeV the additional penetration of the pion, because of the decreased quasielastic absorption, makes this effect more important. It is very possible that the simple form of the potential $(iW\rho^2)$ is inadaquate. A detailed understanding of these data may await more experimental and theoretical studies of the mechanism of pion absorption.
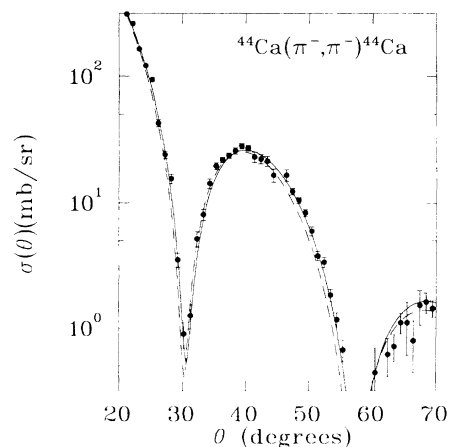

FIG. 5. Sensitivity to a 2% change in the total neutron radius for π^- scattering from ^{44}Ca. The solid curve is for R_n=3.43 fm and the dashed curve for R_n=3.49 fm.

Perhaps the most interesting result from this study is the large valence-neutron radius in ^{42}Ca. It is unfortunate that this result is based on the poorest quality data of the group. The indication is clear that a new experiment with higher quality data is needed.

[1] H. DeVries, C. W. DeJager, and C. DeVries, At. Data Nucl. Data Tables **36**, 495 (1987).

[2] A. Andl, K. Bekk, S. Goring, A. Hanser, G. Nowicki, H. Rebel, G. Schatz, and R. C. Thompson, Phys. Rev. C **26**, 2194 (1982).

[3] I. Talmi, Nucl. Phys. A **423**, 189 (1984).

[4] I. Brissaud and X. Campi, Phys. Lett. **86B**, 141 (1979).

[5] H. J. Gils, E. Friedman, Z. Maika, and H. Rebel, Phys. Rev. C **21**, 1239 (1980).

[6] K. G. Boyer et al., Phys. Rev. C **29**, 182 (1984); K. G. Boyer, thesis, Univerity of Texas, 1983, LA-9974-T.

[7] W. Bertozzi, J. Friar, J. Heisenberg, and J. W. Negele, Phys. Lett. **41B**, 408 (1972).

[8] This independent particle density has been used by many authors. See R. C. Barrett and Daphne F. Jackson, Nuclear Sizes and Structure (Clarendon, Oxford, 1977), for a discussion.

[9] W. B. Kaufmann and W. R. Gibbs, Phys. Rev. C **28**, 1286 (1983).

[10] C. Schmit, Nucl. Phys. A **197**, 449 (1972); J. Revai, ibid. **205**, 20 (1973); C. Schmit, J.-P. Dedonder, and J.-P. Maillet, ibid. **239**, 445 (1975); J.-P. Maillet, J.-P. Dedonder, and C. Schmit, ibid. **271**, 253 (1976); **316**, 267 (1979); M. Silver and N. Austern, Phys. Rev. C **21**, 272 (1980); H. Garcilazo and W. R. Gibbs, Nucl. Phys. A **356**, 284 (1981); **381**, 487 (1982); J. de Kam, Phys. Rev. C **24**, 1544 (1981).

[11] M. J. Leitch, H. W. Baer, R. L. Burman, C. L. Morris, J. N. Knudson, J. R. Comfort, D. H. Wright, R. Gilman, S. H. Rokni, E. Piasetzky, Z. Weinfeld, W. R. Gibbs, and W. B. Kaufmann, Phys. Rev. C **39**, 2356 (1989).

[12] J.-P. Dedonder, J.-P. Maillet, and C. Schmit, Ann. Phys. **127**, 1 (1980).

[13] F. Cannata, J.-P. Dedonder, and W. R. Gibbs, Phys. Rev. C **41**, 1637 (1990).

[14] J.-P. Dedonder and W. R. Gibbs, contributed paper III-70 to PANIC XII, International Conference on Particles and Nuclei, MIT, 1990 (unpublished).

[15] N. Auerbach, J. Bartel, and G. Wenes, Phys. Rev. C **38**, 2921 (1988).

[16] J. Dechargé and D. Gogny, Phys. Rev. C **21**, 1568 (1980).

[17] J. W. Negele and D. Vautherin, Phys. Rev. C **5**, 1472 (1972).

[18] L. Ray, Phys. Rev. C **41**, 2816 (1990).

[19] A. B. Migdal, Yad. Fiz. **16**, 427 (1972) [Sov. J. Nucl. Phys. **16**, 238 (1973)].

[20] P. G. Hansen and B. Jonson, Europhysics Lett. **4**, 409 (1987); L. Johannsen, A. S. Jensen, and P. G. Hansen, Phys. Lett. B **244**, 357 (1990).

[21] G. F. Bertsch, B. A. Brown, and H. Sagawa, Phys. Rev. C **39**, 1154 (1989).

[22] Y. Tosaka and Y. Suzuki, Nucl. Phys. A **512**, 46 (1990).

[23] I. Tanihata, H. Hamagaki, O. Hasimoto, Y. Shida, N. Yoshikawa, K. Sugimoto, O. Yamakawa, T. Kobayashi, and N. Takahashi, Phys. Rev. Lett. **55**, 2676 (1985).

[24] T. Kobayashi, S. Shimoura, I. Tanihata, K. Katori, K. Matsuta, T. Minamisono, K. Sugimoto, W. Muller, D. L. Olsen, T. J. M. Symons, and H. Wieman, Phys. Lett. B **232**, 51 (1989).

[25] R. Anne et al., Phys. Lett. B **250**, 19 (1990).

[26] T. Kobayashi, in Proceedings of the International Workshop on Pions in Nuclei, Penýscola, Spain, 1991, edited by E. Oset, M. J. Vicente Vacas, and C. García Recio (World Scientific, Singapore, 1992), p. 58.

[27] W. R. Gibbs and A. C. Hayes, Phys. Rev. Lett. **67**, 1395 (1991).

[28] S. J. Greene et al., Phys. Rev. C **25**, 927 (1982); K. K. Seth, S. Iverson, H. Nann, M. Kaletka, and J. Hird, Phys. Rev. Lett. **43**, 1574 (1979); **45**, 147 (1980).

[29] K. K. Seth, Nucl. Phys. A **434**, 287c (1985).

[30] L. Ray, Phys. Rev. C **19**, 1855 (1979).

[31] A. Chaumeaux, V. Layly, and R. Schaeffer, Phys. Lett. **72B**, 33 (1977).

[32] D. Vautherin and D. M. Brink, Phys. Rev. C **5**, 626 (1972).

[33] C. J. Batty, E. Friedman, H. J. Gils, and H. Rebel, Advances in Nuclear Physics (Plenum, New York, 1989), Vol. 19, p. 1.